World Journal of Gastroenterology

Submit a Manuscript: http://www.wjgnet.com/esps/
Help Desk: http://www.wjgnet.com/esps/helpdesk.aspx
DOI: 10.3748/wjg.v22.i24.5520

World J Gastroenterol 2016 June 28; 22(24): 5520-5531
ISSN 1007-9327 (print) ISSN 2219-2840 (online)

ORIGINAL ARTICLE

Basic Study

Intravoxel incoherent motion diffusion-weighted imaging for monitoring chemotherapeutic efficacy in gastric cancer

Xiao-Li Song, Heoung Keun Kang, Gwang Woo Jeong, Kyu Youn Ahn, Yong Yeon Jeong, Yang Joon Kang, Hye Jung Cho, Chung Man Moon

Xiao-Li Song, Heoung Keun Kang, Yong Yeon Jeong, Yang Joon Kang, Department of Radiology, Chonnam National University Medical School, Chonnam National University Hwasun Hospital, Hwasun, Jeollanam-do 519-763, South Korea

Gwang Woo Jeong, Chung Man Moon, Department of Radiology, Chonnam National University Medical School, Chonnam National University Hospital, Gwangju 501-757, South Korea

Kyu Youn Ahn, Hye Jung Cho, Department of Anatomy, Chonnam National University Medical School, Gwangju 501-746, South Korea

Author contributions: Song XL and Jeong YY designed the studies; Song XL, Kang YJ and Moon CM performed the majority of experiments; Song XL, Ahn KY, Kang YJ and Cho HJ contributed to the analysis and interpretation of imaging date and histological examination; Song XL wrote the first draft of the manuscript; Jeong GW and Kang HK have approved the final manuscript and completed manuscript; Also, all authors agree with the content of the manuscript.

Supported by National Research Foundation of South Korea, No. NRF-2013R1A1A2013878 and No. 2015R1A2A2A01007827.

Institutional animal care and use committee statement: All procedures involved animals were reviewed and approved by the Institutional Animal Care and Use Committee of the Chonnam National University [CNU IACUC-H-2015-41].

Conflict-of-interest statement: The authors declared that they have no conflicts of interest to this work.

Data sharing statement: No additional data are available.

Correspondence to: Heoung Keun Kang, MD, Professor of Medicine, Department of Radiology, Chonnam National University Medical School, Chonnam National University Hwasun Hospital, Hwasun, Jeollanam-do 519-763, South Korea. hkkang@jnu.ac.kr
Telephone: +82-61-3797101
Fax: +82-61-3797133

Received: February 24, 2016
Peer-review started: February 25, 2016
First decision: March 31, 2016
Revised: April 12, 2016
Accepted: April 20, 2016
Article in press: April 20, 2016
Published online: June 28, 2016

Abstract

AIM: To assess intravoxel incoherent motion diffusion-weighted imaging (IVIM-DWI) for monitoring early efficacy of chemotherapy in a human gastric cancer mouse model.

METHODS: IVIM-DWI was performed with 12 *b*-values (0-800 s/mm^2) in 25 human gastric cancer-bearing nude mice at baseline (day 0), and then they were randomly divided into control and 1-, 3-, 5- and 7-d treatment groups (n = 5 per group). The control group underwent longitudinal MRI scans at days 1, 3, 5 and 7, and the treatment groups underwent subsequent MRI scans after a specified 5-fluorouracil/calcium folinate treatment. Together with tumor volumes (TV), the apparent diffusion coefficient (ADC) and IVIM parameters [true water molecular diffusion coefficient (D), perfusion fraction (f) and pseudo-related diffusion coefficient (D*)] were measured. The differences in

those parameters from baseline to each measurement (ΔTV%, ΔADC%, ΔD%, Δf% and ΔD*%) were calculated. After image acquisition, tumor necrosis, microvessel density (MVD) and cellular apoptosis were evaluated by hematoxylin-eosin (HE), CD31 and terminal-deoxynucleotidyl transferase mediated nick end labeling (TUNEL) staining respectively, to confirm the imaging findings. Mann-Whitney test and Spearman's correlation coefficient analysis were performed.

RESULTS: The observed relative volume increase (ΔTV%) in the treatment group were significantly smaller than those in the control group at day 5 ($\Delta TV_{treatment}\%$ = 19.63% ± 3.01% and $\Delta TV_{control}\%$ = 83.60% ± 14.87%, P = 0.008) and day 7 ($\Delta TV_{treatment}\%$ = 29.07% ± 10.01% and $\Delta TV_{control}\%$ = 177.06% ± 63.00%, P = 0.008). The difference in ΔTV% between the treatment and the control groups was not significant at days 1 and 3 after a short duration of treatment. Increases in ADC in the treatment group ($\Delta ADC\%_{treatment}$, median, 30.10% ± 18.32%, 36.11% ± 21.82%, 45.22% ± 24.36%) were significantly higher compared with the control group ($\Delta ADC\%_{control}$, median, 4.98% ± 3.39%, 6.26% ± 3.08%, 9.24% ± 6.33%) at days 3, 5 and 7 (P = 0.008, P = 0.016, P = 0.008, respectively). Increases in D in the treatment group ($\Delta D\%_{treatment}$, median 17.12% ± 8.20%, 24.16% ± 16.87%, 38.54% ± 19.36%) were higher than those in the control group ($\Delta D\%_{control}$, median -0.13% ± 4.23%, 5.89% ± 4.56%, 5.54% ± 4.44%) at days 1, 3, and 5 (P = 0.032, P = 0.008, P = 0.016, respectively). Relative changes in f were significantly lower in the treatment group compared with the control group at days 1, 3, 5 and 7 follow-up (median, -34.13% ± 16.61% *vs* 1.68% ± 3.40%, P = 0.016; -50.64% ± 6.82% *vs* 3.01% ± 6.50%, P = 0.008; -49.93% ± 6.05% *vs* 0.97% ± 4.38%, P = 0.008, and -46.22% ± 7.75% *vs* 8.14% ± 6.75%, P = 0.008, respectively). D* in the treatment group decreased significantly compared to those in the control group at all time points (median, -32.10% ± 12.22% *vs* 1.85% ± 5.54%, P = 0.008; -44.14% ± 14.83% *vs* 2.29% ± 10.38%, P = 0.008; -59.06% ± 19.10% *vs* 3.86% ± 5.10%, P = 0.008 and -47.20% ± 20.48% *vs* 7.13% ± 9.88%, P = 0.016, respectively). Furthermore, histopathologic findings showed positive correlations with ADC and D and tumor necrosis (r_s = 0.720, P < 0.001; r_s = 0.522, P = 0.007, respectively). The cellular apoptosis of the tumor also showed positive correlations with ADC and D (r_s = 0.626, P = 0.001; r_s = 0.542, P = 0.005, respectively). Perfusion-related parameters (f and D*) were positively correlated to MVD (r_s = 0.618, P = 0.001; r_s = 0.538, P = 0.006, respectively), and negatively correlated to cellular apoptosis of the tumor (r_s = -0.550, P = 0.004; r_s = -0.692, P < 0.001, respectively).

CONCLUSION: IVIM-DWI is potentially useful for predicting the early efficacy of chemotherapy in a human gastric cancer mouse model.

Key words: Gastric cancer; Microvessel density; Nude mouse model; Intravoxel incoherent motion diffusion-weighted imaging; Terminal-deoxynucleoitidyl transferase mediated nick end labeling

Core tip: Intravoxel incoherent motion diffusion-weighted imaging (IVIM-DWI) is useful for monitoring changes of molecular diffusion and microcirculation in gastric cancer at the early stage of chemotherapy. The apparent diffusion coefficient (ADC) and IVIM parameters of true water molecular diffusion coefficient (D) could be reliable marker to detect the necrosis and cellular apoptosis, while perfusion-related IVIM parameters of perfusion fraction (f) and pseudo-related diffusion coefficient (D*) are capable of noninvasive assessment of angiogenesis activity in gastric cancer undergoing chemotherapy.

Song XL, Kang HK, Jeong GW, Ahn KY, Jeong YY, Kang YJ, Cho HJ, Moon CM. Intravoxel incoherent motion diffusion-weighted imaging for monitoring chemotherapeutic efficacy in gastric cancer. *World J Gastroenterol* 2016; 22(24): 5520-5531 Available from: URL: http://www.wjgnet.com/1007-9327/full/v22/i24/5520.htm DOI: http://dx.doi.org/10.3748/wjg.v22.i24.5520

INTRODUCTION

Gastric cancer (GC) remains the fourth most common malignancy and the second-leading cause of cancer deaths in the world[1]. Despite many advances in cancer diagnosis and treatment, approximately two-thirds of patients are diagnosed with advanced gastric cancer (AGC) in many countries, excluding some trial results in Japanese and South Korean patients[2,3]. For many years, 5-fluorouracil (5-FU)-based chemotherapy has been considered a standard chemotherapy regimen for AGC[2-4]. Unfortunately, not all patients benefit from this regimen. If an ineffective therapy can be identified at an early stage of treatment, there will be an opportunity to change the therapy approach and clinical management in the individual patient quickly. The response evaluation criteria in solid tumors (RECIST) is widely adopted standard for evaluating therapy response based on the change in tumor size in clinical practice. However, this often takes several weeks to months to develop, and its evaluation period is too long to adjust patient management[5]. Therefore, increasing demands are being placed on imaging modalities to identify early and reliable surrogate markers for the evaluation of therapeutic effect in patients with GC[6].

Diffusion-weighted magnetic resonance imaging

(DWI) is capable of providing an apparent diffusion coefficient (ADC), which is a measure magnitude of diffusion (of water molecules) within tissue, and has become a favorite choice for oncologic studies[7]. It is well known that a lower ADC is a characteristic of most tumors compare with native tissues because of their high cellularity. An increase in tissue diffusivity, which is induced by an enlarged extracellular space, cell swelling or a loss of membrane integrity under an effective therapy, makes it possible to use ADC to identify the treatment response[8-11]. However, the ADC value derived from DWI based a mono-exponential model does not sufficiently demonstrate the characteristics of tissue behavior. The *b*-value, which represents the strength and timing of the gradients, determines DWI sensitivity to water motion. When a lower *b*-value is applied ($\leqslant$ 100 s/mm^2), microcirculation related protons have relative large diffusion distances, and are capable of changing diffusion signal intensities. In 1986, Le Bihan *et al*[12] first described the concept of intravoxel incoherent motion (IVIM), which can be used to estimate molecular diffusion and microcirculation in the capillaries separately through bi-exponential fitting of the DWI data using multiple *b*-values. In recent years, there has been increasing interests in IVIM-DWI, which allows acquisition of quantitative parameters that reflect tissue diffusivity and microcirculation perfusion simultaneously. The true water molecular diffusion coefficient (D), perfusion fractional (f) volume reflective of capillary blood volume and pseudo-related diffusion coefficient associated with capillary network blood flow (D*) can be measured using IVIM-DWI. The blood microcirculation within capillaries can be considered as a type of "pseudo-diffusion" because it has no specific orientation[13].

It has been determined that IVIM-DWI can provide a new opportunity to gain an insight into the perfusion of a tumor without contrast agent administration for preclinical and clinical applications[12,14,15]. Koh *et al*[16] reported that the calculated f values were lower in colorectal liver metastases, which are characterized by their hypovascular nature, than in the normal liver. In addition, DWI with 10 *b*-values between 0 and 700 s/mm^2 enables the measurement of diffusion and microcirculation contributions in renal allografts as early as 5-d after transplantation[17]. Moreover, IVIM-DWI has been used to evaluate the treatment responses to radiofrequency ablation[18] or a vascular disrupting agent of CKD-516[19] in rabbit model with VX2 liver tumors, and to neoadjuvant chemotherapy in human locoregionally advanced nasopharyngeal carcinoma. Although DWI is increasingly being applied in the body, few studies have focused on gastric lesions due to the limitations of modality of the gastric[20]. Recently, Cheng *et al*[21] applied IVIM with *b*-values of up to 1500 s/mm^2 to evaluate chemotherapeutic efficacy in a gastric cancer xenograft model. In that study, f increased after chemotherapy treatment, which refutes currents theories regarding angiogenesis activity within tumors after treatment[22]. A previous IVIM study in prostate cancer also found that f in tumors significantly increased compared to that in normal prostate tissue when a *b*-value of less than 750 s/mm^2 was used, while f decrease or became indistinguishable from the normal prostate tissue when high *b*-values were employed[23]. This phenomenon could be explained by the following theory: The departure of molecular diffusion at very high *b*-values may have an influence on perfusion-related parameters because both water diffusion and microcirculation contribute to the signal attenuation observed at lower *b*-values ($\leqslant$ 100 s/mm^2)[13,15]. It should be noted that higher b values may affect the accuracy of the IVIM-derived parameters, which depend heavily on the *b*-value selection.

Here, we investigate IVIM-DWI with *b*-values below 800 s/mm^2 as a potential imaging marker for assessing the early chemotherapy response in term of tissue diffusion and microvascular perfusion, by comparing the tissue cellularity and microvascular density (MVD) properties revealed by histopathological analysis during the full course of treatment using a mouse human gastric cancer xenograft model.

MATERIALS AND METHODS

Animal model

This study included 25 male adult (6 weeks old) nude mice (BALB/c-nu/nu, Orient Bio, Gwangju, South Korea), each weighing 20-25 g. All mice, fed with a standard diet with water ad libitum, were maintained in appropriate laboratory conditions (a photoperiod of 12 h light and darkness, 50% humidity, 23 ℃). After a two-week adaption period, 1 × 10^7 human gastric adenocarcinoma AGS cells (ATCC®, CRL-1739™) suspended in 100 μL cold PBS were subcutaneously injected into the lower right hind limbs of the nude mice with a 31 gauge syringe. To evaluate the therapeutic response, the tumor growth curves in each group were estimated based on the morphologic T2-weighted images by using the following formula: TV = π/6 × L × W × H (L, length, W, width, H, height of the tumor).

Study design

Following a baseline (day 0) MRI examination, human gastric cancer-bearing mice were randomly divided into control and 1-d, 3-d, 5-d, and 7-d treatment groups (n = 5 per group). 5-fluorouracil (5-FU) (15 mg/kg)/calcium folinate (5 mg/kg) was used for chemotherapy in the treatment groups, while same volume of saline was administered in the control group. 5-FU/calcium folinate was intraperitoneally injected on a bi-daily basis. Mice in the control group underwent longitudinal MRI at days 1, 3, 5 and 7. Each treatment group underwent a second scan with same MRI protocol at days 1, 3, 5, or 7 after treatment. After the MRI examination, mice were euthanized by an

overdose of isoflurane, and the tumor was stripped for further analysis. The short-term 7-d 5-FU treatment was performed, because this study was aimed to investigate the potential of IVIM-DWI for monitoring the early tumor diffusion and perfusion response to treatment.

MRI protocol

All MRI scans were performed using 3T MRI (GE Healthcare, Waukesha, WI, United States) with a wrist coil. Mice were placed on a heated pad and anesthetized with 2% isoflurane in oxygen (at a rate of 1.0 L/min) to void movement during imaging. After acquisition of the routine images for localization, a transverse T2-weighted image was obtained using fast spin echo (FSE) sequence [repetition time/echo time (TR/TE), 2000/99.6 ms; section thickness, 3 mm; matrix, 512 × 358; number of excitations (NEX), 4]. Subsequently, IVIM-DWI with 12 *b*-values (0, 10, 15, 20, 25, 30, 60, 75, 100, 200, 400 and 800 s/mm^2) were acquired using a free-breathing single-shot echo-planar imaging (EPI) sequence with application of three diffusion-gradients directions (TR/TE, 2500/66.5; section thickness, 3 mm; number of sections, 8; field of view, 10 × 10 cm^2; matrix, 128 × 128; NEX, 4) with an acquisition time of 7 min and 30 s for each study.

MR imaging analysis

The acquired datasets were transferred to a GE workstation (Advance Workstation 4.6) and analyzed using an in-house software. The ADC value was calculated by using a liner fit (least-squares fit) mono-exponential model based on the following equation: $S_b/S_0 = \exp(-b \times ADC)$[15], where S_0 is the signal intensity at a *b* value of 0 and S_b is the signal intensity at higher *b* values. IVIM parameters was calculated by a nonlinear fit (Levenberg-Marquardt fit)bi-exponential model, and the equation is shown as follow: $S_b/S_0 = (1-f) \times \exp(-bD) + f \times \exp[-b(D + D^*)]$[15], where D represents true water molecular diffusion coefficient, f and D* represent perfusion fraction and pseudo-related diffusion coefficient, respectively. A technician with 8 years of experience in MRI measured the tumor sizes and values of ADC, D, f, and D*. The technician was blinded to the information regarding the treatment and control groups.

Regions of interest (ROIs) were drawn by outlining the tumor border on ADC maps, which showed the largest cross-section of the tumor. The ROIs on ADC map were copied and pasted on the corresponding D, f, and D* maps. In each mouse, the change in tumor volume (TV) relative to the baseline was quantified to determine the treatment response as follows: $\Delta TV\% = [(TV_{given\ time} - TV_{baseline})/TV_{baseline}] \times 100$, where $TV_{given\ time}$ is the tumor volume on day 1, 3, 5, or 7 and $TV_{baseline}$ is the tumor volume on day 0. For the ADC and IVIM parameters, the percentage changes in values compared to the baseline were recorded by using the following formula: $\Delta Value\% = [(Value_{given\ time} - Value_{baseline})/Value_{baseline}] \times 100$, where $value_{given\ time}$ is the value on day 1, 3, 5, or 7 and $Value_{baseline}$ is the value on day 0.

Histopathological analysis

The tumor tissue was paraffin-embedded, and sliced in the transverse plane at 0.6 μm intervals to match the corresponding MR image, was selected. The necrotic fraction (NF) of the tumor was evaluated through hematoxylin-eosin (HE) staining. CD31 (Dako, Carpinteria, CA, United States; mouse anti-human; used at 1:200) staining was carried out on pathological specimens by immunohistochemical methods, to analyze the angiogenesis activity of the tumor. The paraffin-embedded sections were incubated with the primary antibody at 4 ℃ overnight. Secondary antibody (Stem cell Technologies; rabbit anti-mouse; used at 1:300) was applied at room temperature for 1 h and then sections were rinsed with PBS. Positive reaction was visualized by DAB chromogen (Dako, Carpinteria, CA, United States) according to standard methods. Terminal deoxynucleotidyl transferase dUTP nick end labeling (TUNEL) (Roche Applied Science, Penzberg, Germany) was performed to evaluate cellular apoptosis of the tumor by following the manufacturer's instructions.

Histopathological analysis was performed by using Image J software (http://rsb.info.nih.gov/ij). Tumor necrosis was scored according to the following formula: $NF = Area_{necrosis}/Area_{total\ tumor}$. Cellular apoptosis of the tumor was defined as the percentage of positive TUNEL-stained cells among 200 nuclei from five randomly selected fields at a high magnification (× 200). The mean MVD of the tumor was defined by the CD31-stained vessels[24], where any distinct area of positive for CD31 staining was defined as a single vessel, from five hot spots with higher vascular density compared to the remaining tissue in a high-power field (× 200; 0.578 mm^2).

Statistical analysis

SPSS 21.0 (SPSS, Chicago, IL, United States) was used for statistical analysis. The differences in relative changes in the ADC and IVIM parameters, and tumor volumes between the control and treatment groups were determined by the Mann-Whitney test. Spearman's correlation coefficient was used to determine the correlations between histological features, including NF, MVD and TUNEL and the corresponding ADC and IVIM parameters. Spearman's coefficient was considered to be satisfactory with a critical value of $r_s = 0.415$ at P value < 0.05 (two-tailed test). A spearman's coefficient of 0.90-1.00 indicated almost perfect agreement; 0.70-0.90 indicated high agreement; 0.50-0.70 indicate moderate agreement; 0.30-0.50 indicate low agreement; and 0.00-0.30 indicate negligible agreement[25]. A two-tailed *P* value

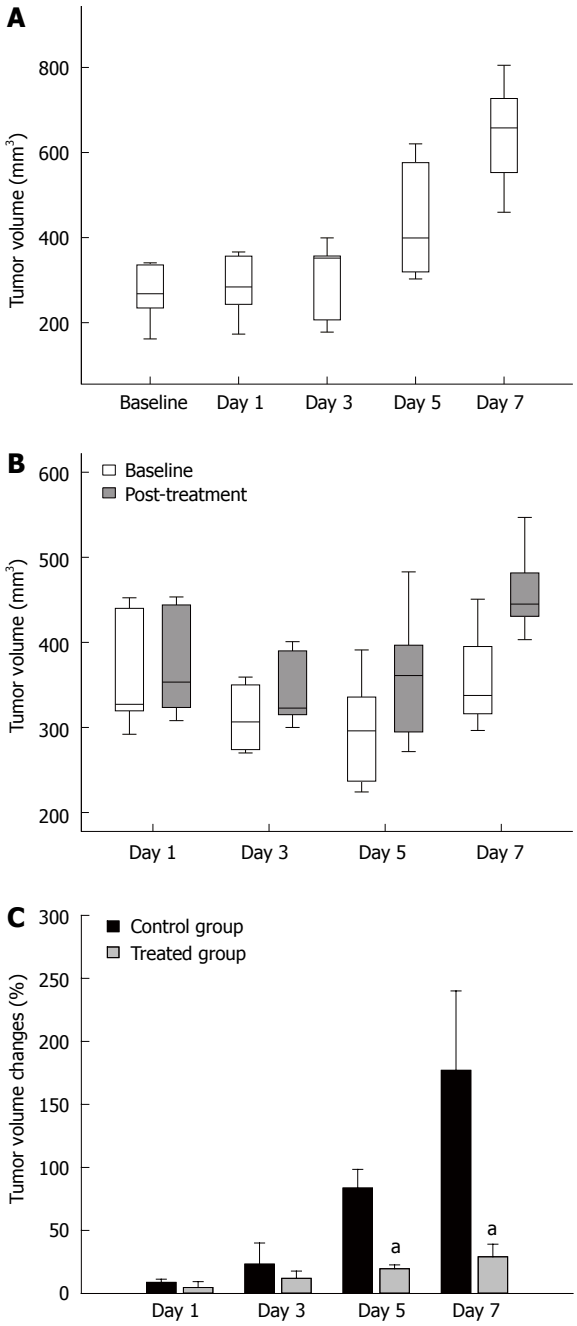

Figure 1 Anti-tumor effects of 5-fluorouracil therapy in mouse gastric cancer xenografts. A: Actual tumor volume changes in the control group; B: Actual tumor volume changes in the treatment groups; C: The comparison of the change in tumor volumes relative to baseline (day 0) between the control and treatment groups. The control group showed increases in tumor volume, while the treatment group showed as significant tumor growth delay from day 5. Center line = median; upper and lower margins of the box = 25th to the 75th percentile, respectively; whiskers = data from the minimum to the maximum. Error bars denote standard errors. $^{a}P < 0.05$ *vs* control group, $n = 5$ in each group.

< 0.05 was considered as significant difference.

RESULTS

Effects of chemotherapy on tumor growth

Twenty-five tumors with a mean volume of 298.07 ± 103.44 mm^3 (range: 194.32-432.34 mm^3) before treatment were analyzed 20 to 25 d of implantation. The tumor volume in the control and treatment groups is shown in Figure 1A and B. 5-FU induced a significant growth delay, as assessed by the MRI-derived tumor volume measurements in comparison with that in the control group from day 5. As shown in Figure 1C, the observed relative volume increase (ΔTV%) in the therapy groups were significantly lower than in the control group at day 5 ($\Delta TV_{treatment}\%$ = 19.63% ± 3.01% and $\Delta TV_{control}\%$ = 83.60% ± 14.87%, $P = 0.008$) and day 7 ($\Delta TV_{treatment}\%$ = 29.07% ± 10.01% and $\Delta TV_{control}\%$ = 177.06% ± 63.00%, $P = 0.008$). The difference in ΔTV% between the treatment and the control groups was not significant at day 1 ($\Delta TV_{treatment}\%$ = 4.97% ± 4.59% and $\Delta TV_{control}\%$ = 8.08% ± 2.47%, $P = 0.841$) or day 3 ($\Delta TV_{treatment}\%$ = 15.36% ± 5.75% and $\Delta TV_{control}\%$ = 23.28% ± 16.76%, $P = 0.310$) after a short treatment duration.

IVIM-DWI assessment of a human gastric cancer xenograft

Table 1 summarizes the ADC, D, f, and D* values of the tumors in the control and treatment groups, that were measured at baseline and at days 1, 3, 5 and 7. Figure 2 shows the mean percentage changes in the DWI parameters relative to baseline at each time point in each group. In the control group, all ADC values and IVIM parameters of the tumor remained relatively constant over the 7-d experiment. ADC increases in the treatment group ($\Delta ADC\%_{treatment}$, median, 30.10% ± 18.32%, 36.11% ± 21.82%, 45.22% ± 24.36%) were significantly higher compared with the control group ($\Delta ADC\%_{control}$, median, 4.98% ± 3.39%, 6.26% ± 3.08%, 9.24% ± 6.33%) at days 3, 5 and 7 ($P = 0.008$, $P = 0.016$, $P = 0.008$, respectively) (Figure 2A). Increases in D in the treatment group ($\Delta D\%_{treatment}$, median 17.12% ± 8.20%, 24.16% ± 16.87%, 38.54% ± 19.36%) were higher than in the control group ($\Delta D\%_{control}$, median -0.13% ± 4.23%, 5.89% ± 4.56%, 5.54% ± 4.44%) at days 1, 3, and 5 ($P = 0.032$, $P = 0.008$, $P = 0.016$, respectively) (Figure 2B). The relative changes in f were significantly lower in the treatment group than in the control group at days 1, 3, 5 and 7 follow-up (median, -34.13% ± 16.61% *vs* 1.68% ± 3.40%, $P = 0.016$; -50.64% ± 6.82% *vs* 3.01% ± 6.50%, $P = 0.008$; -49.93% ± 6.05% *vs* 0.97% ± 4.38%, $P = 0.008$, and -46.22% ± 7.75% *vs* 8.14% ± 6.75%, $P = 0.008$, respectively) (Figure 2C). D* in the treatment group decreased significantly compared with the control group at all time points (median, -32.10% ± 12.22% *vs* 1.85% ± 5.54%, $P = 0.008$; -44.14% ± 14.83% *vs* 2.29% ± 10.38%, $P = 0.008$; -59.06% ± 19.10% *vs* 3.86% ± 5.10%, $P = 0.008$, and -47.20% ± 20.48% *vs* 7.13% ± 9.88%, $P = 0.016$, respectively) (Figure 2D).

Histopathological assessment of tumor response and its correlation with MR images

HE, CD31 and TUNEL staining were performed to

Table 1 Summary of the apparent diffusion coefficient and intravoxel incoherent motion parameters at baseline (day 0) and on days 1, 3, 5, and 7 in each groups (n = 5 per group)

	ADC (10^{-3} mm^2/s)	IVIM parameters		
		D (10^{-3} mm^2/s)	f (%)	D^* (mm^2/s)
Control group				
Day 0	0.514 ± 0.050	0.480 ± 0.049	32.424 ± 6.647	0.112 ± 0.017
Day 1	0.520 ± 0.056	0.497 ± 0.052	33.010 ± 7.121	0.114 ± 0.016
Day 3	0.537 ± 0.029	0.506 ± 0.025	33.606 ± 8.113	0.115 ± 0.020
Day 5	0.545 ± 0.047	0.504 ± 0.021	32.602 ± 6.684	0.117 ± 0.018
Day 7	0.561 ± 0.053	0.524 ± 0.064	35.100 ± 7.858	0.120 ± 0.016
1-d treatment group				
Day 0	0.555 ± 0.028	0.524 ± 0.028	34.076 ± 7.247	0.171 ± 0.049
Day 1	0.597 ± 0.064	0.612 ± 0.065	21.912 ± 5.032	0.115 ± 0.040
3-d treatment group				
Day 0	0.528 ± 0.012	0.510 ± 0.019	37.066 ± 7.331	0.147 ± 0.025
Day 3	0.686 ± 0.107	0.636 ± 0.121	18.596 ± 5.766	0.083 ± 0.029
5-d treatment group				
Day 0	0.594 ± 0.069	0.567 ± 0.065	34.664 ± 8.337	0.173 ± 0.068
Day 5	0.804 ± 0.136	0.777 ± 0.107	17.344 ± 4.352	0.070 ± 0.045
7-d treatment group				
Day 0	0.560 ± 0.060	0.535 ± 0.081	37.598 ± 5.852	0.148 ± 0.082
Day 7	0.823 ± 0.221	0.710 ± 0.236	20.040 ± 3.042	0.065 ± 0.018

ADC: Apparent diffusion coefficient; IVIM: Intravoxel incoherent motion.

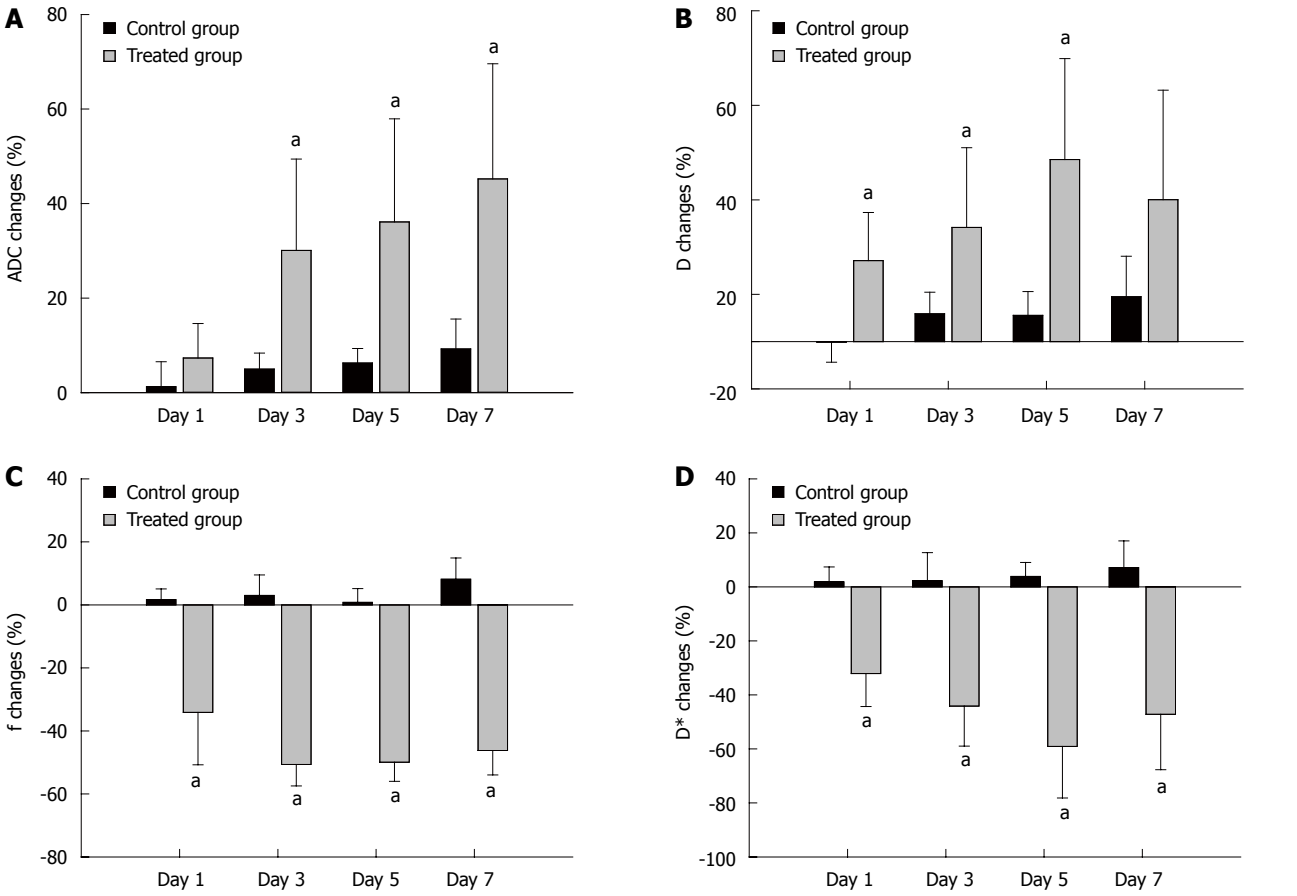

Figure 2 Comparison of the mean percentage changes from baseline in the intravoxel incoherent motion diffusion-weighted imaging derived values between the control (dark) and the 1-, 3-, 5- and 7-d treatment groups (grey). A: ADC value; B: D value; C: f value; D: D* value. Standard deviations are represented by vertical bars. Relative changes were determined by comparing the values at baseline and those in follow-up. $^aP < 0.05$ *vs* control. n = 5 in each group. ADC: Apparent diffusion coefficient.

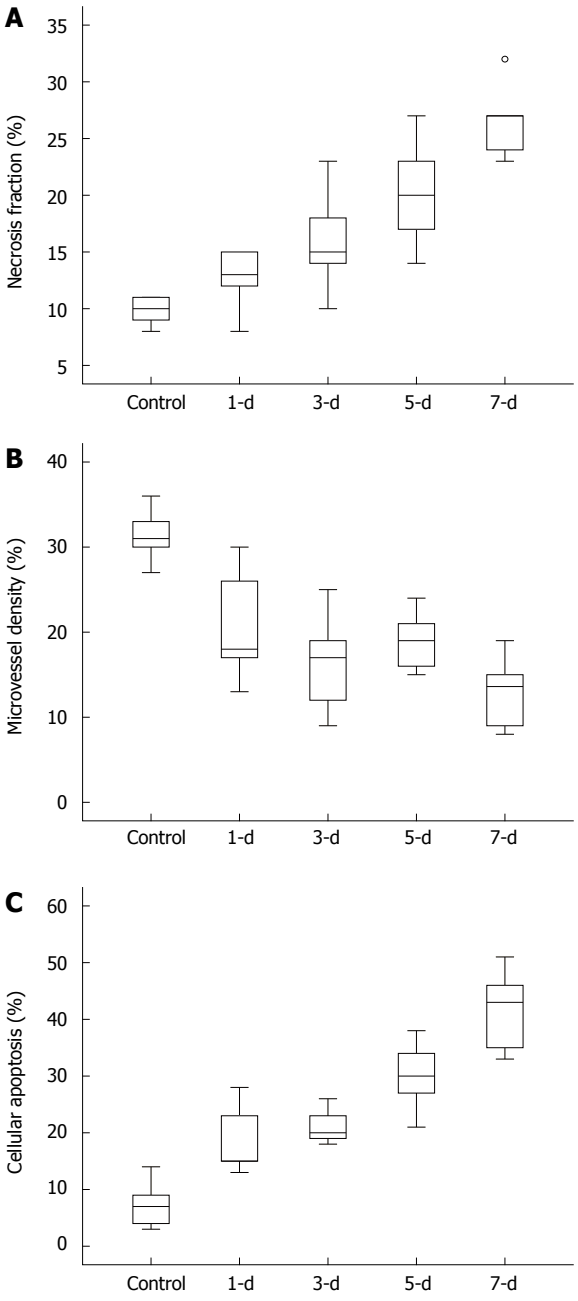

Figure 3 Box-and-Whisker plots show the results of histopathological analysis in the control and the 1-, 3-, 5- and 7-d treatment groups, respectively (*n* = 5 per group). A: Necrosis fraction of tumor; B: Microvessel density of tumor; C: Cellular apoptosis of tumor. Center line = median; upper and lower margins of box = 25th to the 75th percentile, respectively; whiskers = data from the minimum to the maximum; ○ = outlier.

confirm the tissue and vessel changes in the tumor. Figure 3 shows the quantification of the NF, MVD, and cellular apoptosis in all animals of the control and the treatment groups (n = 5 per group). The MVD scores in 5-FU treatment tumors decreased significantly compared with the control group. The 5-FU treated tumors displayed a time-dependent increase in NF and cellular apoptosis compared to those in the control group, indicating an effective therapeutic response.

Table 2 summarizes the relationship among ADC, the IVIM parameters, MVD, cellular apoptosis and necrosis of tumors (n = 25) determined by Spearman's correlation coefficient analysis. ADC and D were positively correlated with NF (r_s = 0.720, P < 0.001; r_s = 0.522, P = 0.007, respectively) (Figure 4A, B) and the cellular apoptosis of the tumor (r_s = 0.626, P = 0.001; r_s = 0.542, P = 0.005, respectively) (Figure 4E, F).There is no significant correlation among ADC, D, and MVD. Perfusion-related parameters f and D* shows positive correlations with MVD (r_s = 0.618, P = 0.001; r_s = 0.538, P = 0.006, respectively) (Figure 4C, D), and a negative correlation with the cellular apoptosis of the tumor (r_s = -0.550, P = 0.004; r_s = -0.692, P < 0.001, respectively) (Figure 4G, H). There is no significant correlation between the perfusion parameters and NF. Figure 5 shows the calculated ADC, D, f, and D* maps and the correspondent histopathologic images from the control and 3 d treated mice.

DISCUSSION

The ADC obtained from conventional DWI has been widely accepted as a marker to monitor the therapeutic efficacy of chemotherapy, radiotherapy or combined therapy with target medicine[26,27]. In recent years, there has been a resurgent interest in IVIM studies, which allows to measure tissue diffusion and perfusion simultaneously. In this study, we performed IVIM-DWI using 12 b-values less than 800 s/mm^2 to monitor the efficacy of chemotherapy in a mouse model of human gastric cancer. A histopathological analysis was carried out to evaluate the tissue cellularity and MVD properties of the tumor.

Our results demonstrated that conventional ADC significantly increased after 3-d of treatment and it showed a positive correlation with the 5-FU induced intratumoral necrosis and cellular apoptosis of the tumor. Papaevangelou *et al*[28] found that ADC changes in the tumor were associated with the induction of a mixture of necrosis and apoptosis after irinotecan treatment. Therefore, ADC could be a reliable marker for detecting the necrotic and apoptotic cell death in gastric cancer patients during treatment. IVIM derived D values that showed a similar trend to ADC, were significantly increased as early as after one day treatment compared with the baseline values. Moreover, HE and TUNEL stain showed that D values were positively correlated with intratumoral necrosis and cellular apoptosis, indicating the possibility of a noninvasive evaluation of necrosis or apoptotic. Our finding regarding the D value is consistent with previous studies which showed that an increase in D value can predict chemotherapeutic responsiveness in locoregionally advanced nasopharyngeal carcinoma[20] and advanced cervical cancer[29]. There is no denying that accurate quantification of the D value, which associates with the intra-to-extracellular spaces ratio

Table 2 Correlation between apparent diffusion coefficient and intravoxel incoherent motion parameters, microvessel density, cellular apoptosis and necrosis fraction of tumors (n = 25)

	NF (%)		MVD (vessels/HPF)		Apoptosis (%)	
	r_s	*P* value	r_s	*P* value	r_s	*P* value
ADC ($\times 10^{-3}$ mm^2/s)	0.720	< 0.001	-0.395	0.051	0.626	0.001
IVIM parameters						
D ($\times 10^{-3}$ mm^2/s)	0.522	0.007	-0.201	0.335	0.542	0.005
f (%)	-0.347	0.089	0.618	0.001	-0.550	0.004
D^* ($\times$ mm^2/s)	-0.378	0.062	0.538	0.006	-0.692	< 0.001

P < 0.05 is considered to be statistically significant. ADC: Apparent diffusion coefficient; IVIM: Intravoxel incoherent motion; MVD: Microvessel density; NF: Necrosis fraction.

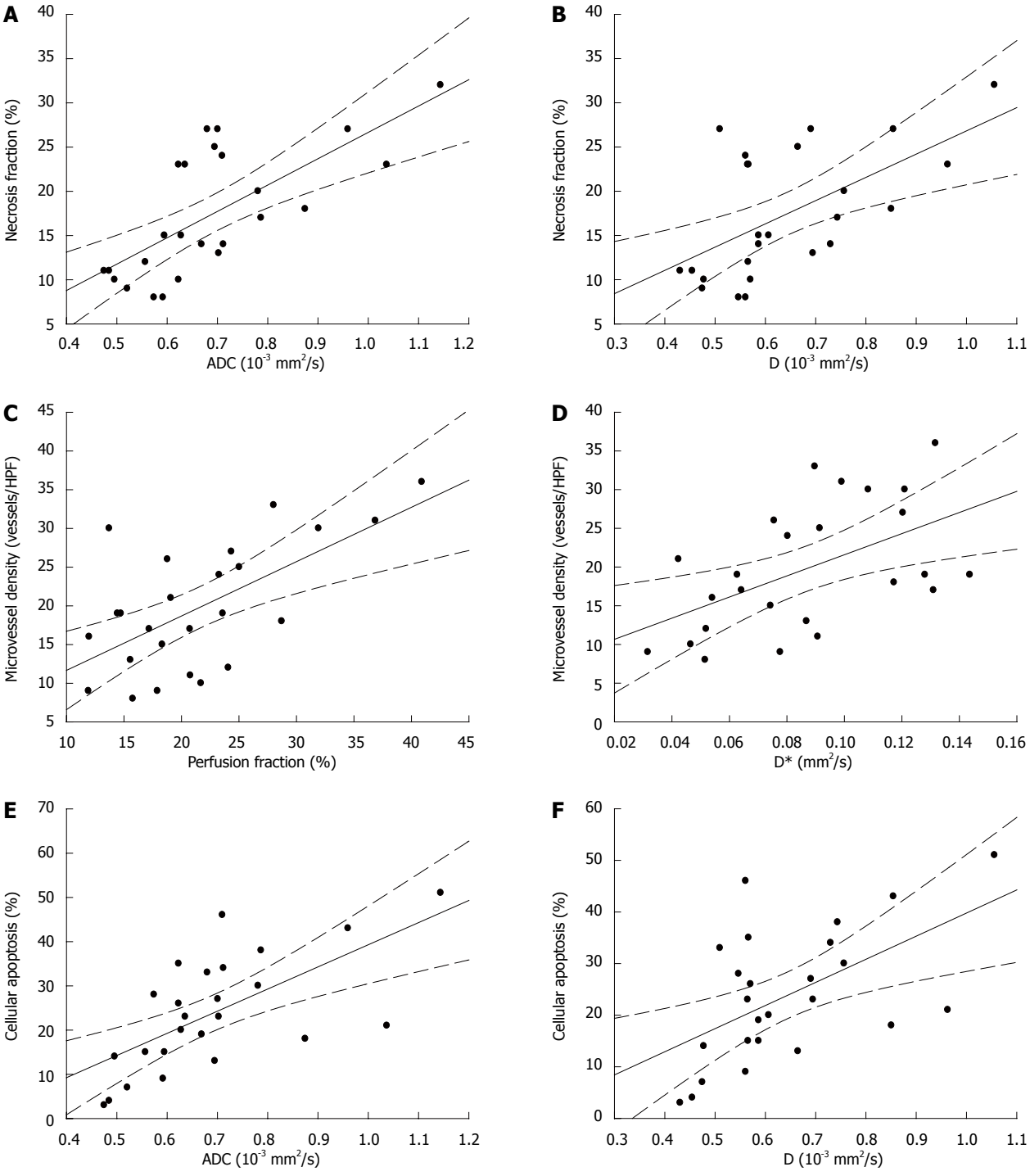

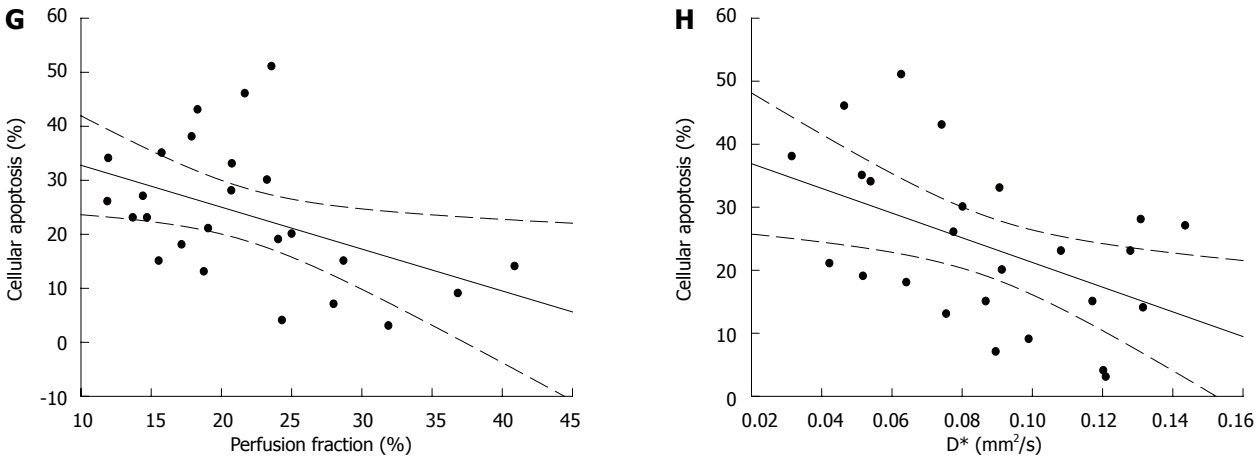

Figure 4 Representative scatter diagrams showing the relationships between intravoxel incoherent motion diffusion-weighted imaging derived parameters and the histological features (*n* = 25). A and B: ADC and D were positively correlated with tumor necrosis fraction; C and D: f and D* were positively correlated with microvascular density of tumor; E and F: ADC, D were positively correlated with tumor cellular apoptosis; G and H: f and D* were negatively correlated with tumor cellular apoptosis. *P* values are shown in Table 2. ADC: Apparent diffusion coefficient.

and represents the true molecular diffusion, would eventually translate into a reliable marker to evaluate the tumor therapy response.

The f and D* significantly decreased during the early phase of chemotherapy. In addition, the f and D* were well correlated with the decrease in MVD revealed by the endothelial cell marker CD31 staining, which indicated that f and D* have the potential to assess tumor angiogenesis activity noninvasively. There are experimental and clinical dates in body tissues with IVIM-DWI which support the claim that the signal attenuation is related to microcirculation in tissue when *b*-values less than 100 s/mm^2 were applied. Wang *et al*[30] found an increase in the tumor blood flow induced by IV hydralazine injection was accompanied by an increase in the IVIM-derived D* in a mammary adenocarcinoma rat model. In a human brain study, f and D* were correlated separately with the relative blood volume and blood flow derived from dynamic susceptibility contrast enhancement imaging[31]. Joo *et al*[19] reported that IVIM-DWI has the potential to evaluate the early therapeutic effect induced by a vascular disrupting agent named CKD-516 in rabbit VX2 liver tumors. In addition, f and D* also showed a weak negative correlation with the cellular apoptosis of the tumor, indicating that the decreased cellularity also contributed to the changes in f and D*. This may reconfirm the finding that tissue water diffusion also contributes to the observed signal attenuation at low *b*-values. After effective chemotherapy, extracellular spaces would expand, resulting in less restriction of migration of water molecules and weakening the process of pseudo-diffusion. This would then yield a higher D value and lower f and D* than those obtained pre-treatment. Our results and the conclusions from previous studies[13,32] indicated the usefulness of IVIM-DWI for depicting the therapeutic efficiency in gastric cancer before changes in tumor size are evident.

The option of a bi-exponential model for extracting molecular diffusion and microcirculation perfusion information from DWI remains controversial. A previous IVIM study with the *b*-values up to 1500 s/mm^2 found that f increased after treatment, which contradicts our finding[21]. Pang *et al*[23] found that f obtained from *b*-values below 750 s/mm^2 is more in keeping with the increased perfusion in prostate cancer tissue, while f decrease or became indistinguishable from the normal level of prostate tissue when high *b*-values employed. Both tissue microcirculation and water diffusion in the tissue contributed to signal attenuation at a low *b*-value; hence, departure of molecular diffusion at very high *b*-values may influence the perfusion-related parameters[33,34]. Moreover, the IVIM method suffers significantly from the variations in the signal-to-noise ratio and is prone to generate measurement errors when *b*-values are lower than 100 s/mm^2[13]. To date, no consensus has been reached on the magnitude and number of *b*-values that ought to be applied in preclinical and clinical studies. Therefore, more studies are required to optimize the process of image collection and image post-processing for deriving sufficiently accurate parameters based on the original IVIM model.

There are limitations to this study. First, the observation endpoint in this study is too short. Secondly, because of the small sample sizes, serial relative changes in ADC and the IVIM parameters of the tumor were not evaluated in the treatment groups. Therefore, we need further studies with larger sample size and long-term observations to clarity the limitation of this study.

In conclusion, IVIM-DWI raises the possibility of an effective, multi-parametric (D, f, D*) imaging method without requirement of gadolinium enhancement. The IVIM method could potentially be used to assess tissue diffusivity changes in addition to evaluate the microcirculatory perfusion of gastric cancer in response

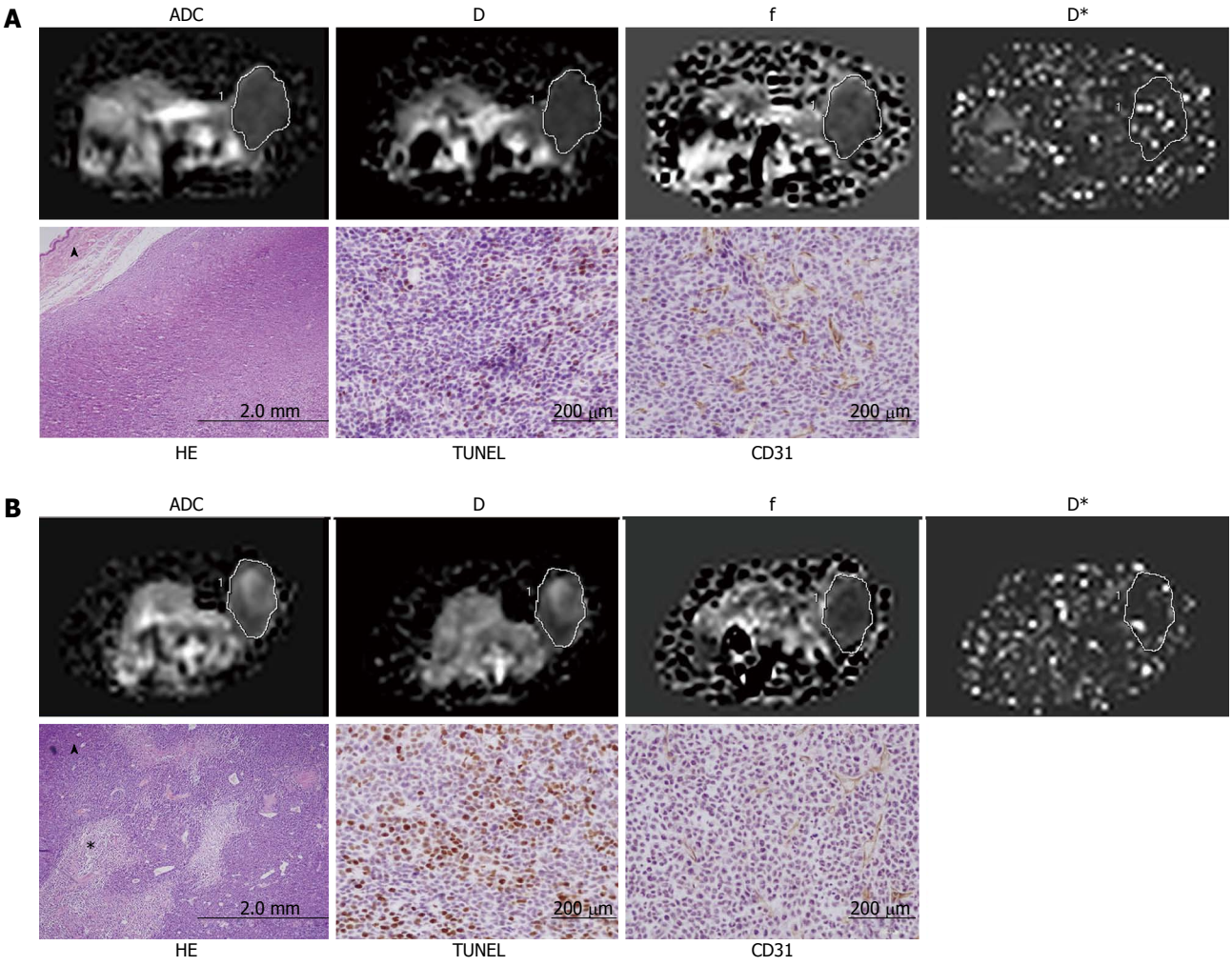

Figure 5 Calculated maps of intravoxel incoherent motion diffusion-weighted imaging parameters and the histopathological images. A: The lower ADC (0.521 × 10^{-3} mm^2/s) and D values (0.475 × 10^{-3} mm^2/s) and the higher f (40.92%) and D* (0.131 mm^2/s) values, which correspond to low necrosis (10%) and cellular apoptosis (7%) and high MVD (36) in the control group; B: Increased ADC (0.875 × 10^{-3} mm^2/s) and D (0.851 × 10^{-3} mm^2/s) values and reduced f (17.20%) and D* (0.098 mm^2/s) values, which correspond to the increased necrosis (18%) and cellular apoptosis (23%) and decreased MVD (17) in the 3-d treatment group. Note high signal intensity within tumor suggesting necrosis. asterisk means necrosis area; The triangle symbol means skin of the mouse. ADC: Apparent diffusion coefficient; MVD: Microvessel density.

to chemotherapy.

ACKNOWLEDGMENTS

The authors thank Mr. Kim Don Geun GE Healthcare for magnetic resonance imaging technical support and Pro of Moon Jai Dong Chonnam National University Medical School for advice on statistic analysis.

COMMENTS

Background

Chemotherapy is a standard treatment for advanced gastric cancer. Imaging modalities that help to identify early and reliable surrogate markers for the evaluation of chemotherapy response are important in patients with gastric cancer. Intravoxel incoherent motion diffusion-weighted imaging (IVIM-DWI), which allows acquisition of quantitative parameters that reflect tissue diffusivity and tissue microcapillary perfusion, maybe a useful tool that can monitor the early chemotherapy response in terms of gastric cancer tissue diffusion and microvascular perfusion.

Research frontiers

IVIM-DWI has been used to monitor the treatment responses to radiofrequency ablation or a vascular disrupting agent of CKD-516 in rabbit model with VX2 liver tumors, and the response of human locoregionally advanced nasopharyngeal carcinoma to neoadjuvant chemotherapy. DWI is increasingly being applied in the human body, but few studies focused on the gastric lesions due to the limitation of the modality.

Innovations and breakthroughs

In this study, IVIM-DWI with 12 *b*-values less than 800 s/mm^2 was performed to avoid the potential impact of higher *b*-values on the accuracy of the IVIM-derived parameters.

Applications

IVIM-DWI raises the possibility of an effective, multi-parametric (D, f, D*) imaging method that does not require gadolinium enhancement. The IVIM method could potentially be used to assess tissue diffusivity changes in addition to measuring the microcirculatory perfusion of gastric cancer in response to

chemotherapy.

Terminology

DWI is capable of providing a parameter of apparent diffusion coefficient (ADC). The measured ADC, which represents tissue diffusivity, has become a favorite choice in oncologic studies. IVIM-DWI allows acquisition of multi-quantitative parameters that reflect tissue diffusivity and microcirculation perfusion.

Peer-review

The authors have demonstrated the usefulness of IVIM-DWI for monitoring early chemotherapeutic efficacy in a human gastric cancer xenograft model with nude mouse. The manuscript presents interesting and novel findings. The data are well presented and important. However, noted by the authors, the limitation of this study is the short observation endpoint.

REFERENCES

1 **Carcas LP**. Gastric cancer review. *J Carcinog* 2014; **13**: 14 [PMID: 25589897 DOI: 10.4103/1477-3163.146506]

2 **Spampatti S**, Rausei S, Galli F, Ruspi L, Peverelli C, Frattini F, Rovera F, Boni L, Dionigi G. Neoadjuvant chemotherapy for locally advanced gastric cancer: the surgeon's role. *Transl Gastrointest Cancer* 2015; **4**: 141-147 [DOI: 10.3978/j.issn.2224-4778.2014.12.02]

3 **Digklia A**, Wagner AD. Advanced gastric cancer: Current treatment landscape and future perspectives. *World J Gastroenterol* 2016; **22**: 2403-2414 [PMID: 26937129 DOI: 10.3748/wjg.v22.i8.2403]

4 **Park SC**, Chun HJ. Chemotherapy for advanced gastric cancer: review and update of current practices. *Gut Liver* 2013; **7**: 385-393 [PMID: 23898376 DOI: 10.5009/gnl.2013.7.4.385]

5 **Therasse P**, Arbuck SG, Eisenhauer EA, Wanders J, Kaplan RS, Rubinstein L, Verweij J, Van Glabbeke M, van Oosterom AT, Christian MC, Gwyther SG. New guidelines to evaluate the response to treatment in solid tumors. European Organization for Research and Treatment of Cancer, National Cancer Institute of the United States, National Cancer Institute of Canada. *J Natl Cancer Inst* 2000; **92**: 205-216 [PMID: 10655437 DOI: 10.1093/jnci/92.3.205]

6 **Sadeghi-Naini A**, Falou O, Hudson JM, Bailey C, Burns PN, Yaffe MJ, Stanisz GJ, Kolios MC, Czarnota GJ. Imaging innovations for cancer therapy response monitoring. *Imaging Med* 2012; **4**: 311-327 [DOI: 10.2217/iim.12.23]

7 **Ross BD**, Moffat BA, Lawrence TS, Mukherji SK, Gebarski SS, Quint DJ, Johnson TD, Junck L, Robertson PL, Muraszko KM, Dong Q, Meyer CR, Bland PH, McConville P, Geng H, Rehemtulla A, Chenevert TL. Evaluation of cancer therapy using diffusion magnetic resonance imaging. *Mol Cancer Ther* 2003; **2**: 581-587 [PMID: 12813138]

8 **Nilsen L**, Fangberget A, Geier O, Olsen DR, Seierstad T. Diffusion-weighted magnetic resonance imaging for pretreatment prediction and monitoring of treatment response of patients with locally advanced breast cancer undergoing neoadjuvant chemotherapy. *Acta Oncol* 2010; **49**: 354-360 [PMID: 20397769 DOI: 10.3109/02841861003610184]

9 **Cui Y**, Zhang XP, Sun YS, Tang L, Shen L. Apparent diffusion coefficient: potential imaging biomarker for prediction and early detection of response to chemotherapy in hepatic metastases. *Radiology* 2008; **248**: 894-900 [PMID: 18710982 DOI: 10.1148/radiol.2483071407]

10 **Siegel MJ**, Jokerst CE, Rajderkar D, Hildebolt CF, Goyal S, Dehdashti F, Wagner Johnston N, Siegel BA. Diffusion-weighted MRI for staging and evaluation of response in diffuse large B-cell lymphoma: a pilot study. *NMR Biomed* 2014; **27**: 681-691 [PMID: 24700565 DOI: 10.1002/nbm.3105]

11 **Wu X**, Kellokumpu-Lehtinen PL, Pertovaara H, Korkola P, Soimakallio S, Eskola H, Dastidar P. Diffusion-weighted MRI in early chemotherapy response evaluation of patients with diffuse large B-cell lymphoma--a pilot study: comparison with 2-deoxy-2-fluoro- D-glucose-positron emission tomography/computed tomography. *NMR Biomed* 2011; **24**: 1181-1190 [PMID: 21387451 DOI: 10.1002/nbm.1689]

12 **Le Bihan D**, Breton E, Lallemand D, Grenier P, Cabanis E, Laval-Jeantet M. MR imaging of intravoxel incoherent motions: application to diffusion and perfusion in neurologic disorders. *Radiology* 1986; **161**: 401-407 [PMID: 3763909 DOI: 10.1148/radiology.161.2.3763909]

13 **Koh DM**, Collins DJ, Orton MR. Intravoxel incoherent motion in body diffusion-weighted MRI: reality and challenges. *AJR Am J Roentgenol* 2011; **196**: 1351-1361 [PMID: 21606299 DOI: 10.2214/AJR.10.5515]

14 **Kang KM**, Lee JM, Yoon JH, Kiefer B, Han JK, Choi BI. Intravoxel incoherent motion diffusion-weighted MR imaging for characterization of focal pancreatic lesions. *Radiology* 2014; **270**: 444-453 [PMID: 24126370 DOI: 10.1148/radiol.13122712]

15 **Le Bihan D**, Breton E, Lallemand D, Aubin ML, Vignaud J, Laval-Jeantet M. Separation of diffusion and perfusion in intravoxel incoherent motion MR imaging. *Radiology* 1988; **168**: 497-505 [PMID: 3393671 DOI: 10.1148/radiology.168.2.3393671]

16 **Koh DM**, Scurr E, Collins DJ, Pirgon A, Kanber B, Karanjia N, Brown G, Leach MO, Husband JE. Colorectal hepatic metastases: quantitative measurements using single-shot echo-planar diffusion-weighted MR imaging. *Eur Radiol* 2006; **16**: 1898-1905 [PMID: 16691378 DOI: 10.1007/s00330-006-0201-x]

17 **Eisenberger U**, Thoeny HC, Binser T, Gugger M, Frey FJ, Boesch C, Vermathen P. Evaluation of renal allograft function early after transplantation with diffusion-weighted MR imaging. *Eur Radiol* 2010; **20**: 1374-1383 [PMID: 20013274 DOI: 10.1007/s00330-009-1679-9]

18 **Guo Z**, Zhang Q, Li X, Jing Z. Intravoxel Incoherent Motion Diffusion Weighted MR Imaging for Monitoring the Instantly Therapeutic Efficacy of Radiofrequency Ablation in Rabbit VX2 Tumors without Evident Links between Conventional Perfusion Weighted Images. *PLoS One* 2015; **10**: e0127964 [PMID: 26020785 DOI: 10.1371/journal.pone.0127964]

19 **Joo I**, Lee JM, Han JK, Choi BI. Intravoxel incoherent motion diffusion-weighted MR imaging for monitoring the therapeutic efficacy of the vascular disrupting agent CKD-516 in rabbit VX2 liver tumors. *Radiology* 2014; **272**: 417-426 [PMID: 24697148 DOI: 10.1148/radiol.14131165]

20 **Xiao Y**, Pan J, Chen Y, Chen Y, He Z, Zheng X. Intravoxel Incoherent Motion-Magnetic Resonance Imaging as an Early Predictor of Treatment Response to Neoadjuvant Chemotherapy in Locoregionally Advanced Nasopharyngeal Carcinoma. *Medicine* (Baltimore) 2015; **94**: e973 [PMID: 26091468 DOI: 10.1097/MD.0000000000000973]

21 **Cheng J**, Zhang C, Wang H, Wu W, Pan F, Hong N, Wang Y. Evaluation of chemotherapy response of gastric cancer in a mouse model using intravoxel incoherent diffusion-weighted MRI correlated with histopathological characteristics. *ECR* 2015; C-0536 [DOI: 10.1594/ecr2015/C-0536]

22 **Ma J**, Waxman DJ. Combination of antiangiogenesis with chemotherapy for more effective cancer treatment. *Mol Cancer Ther* 2008; **7**: 3670-3684 [PMID: 19074844 DOI: 10.1158/1535-7163.MCT-08-0715]

23 **Pang Y**, Turkbey B, Bernardo M, Kruecker J, Kadoury S, Merino MJ, Wood BJ, Pinto PA, Choyke PL. Intravoxel incoherent motion MR imaging for prostate cancer: an evaluation of perfusion fraction and diffusion coefficient derived from different b-value combinations. *Magn Reson Med* 2013; **69**: 553-562 [PMID: 22488794 DOI: 10.1002/mrm.24277]

24 **Weidner N**, Semple JP, Welch WR, Folkman J. Tumor angiogenesis and metastasis--correlation in invasive breast carcinoma. *N Engl J Med* 1991; **324**: 1-8 [PMID: 1701519 DOI: 10.1056/NEJM199101033240101]

25 **Hinkle DE**, Wiersma W, Jurs SG. Applied statistics for the behavioral sciences. 5th ed. Boston: Houghton Mifflin, 2003: 89-90

26 **Woodhams R**, Matsunaga K, Iwabuchi K, Kan S, Hata H, Kuranami M, Watanabe M, Hayakawa K. Diffusion-weighted imaging of malignant breast tumors: the usefulness of apparent

diffusion coefficient (ADC) value and ADC map for the detection of malignant breast tumors and evaluation of cancer extension. *J Comput Assist Tomogr* 2005; **29**: 644-649 [PMID: 16163035 DOI: 10.1097/01.rct.0000171913.74086.1b]

27 **Langer DL**, van der Kwast TH, Evans AJ, Trachtenberg J, Wilson BC, Haider MA. Prostate cancer detection with multi-parametric MRI: logistic regression analysis of quantitative T2, diffusion-weighted imaging, and dynamic contrast-enhanced MRI. *J Magn Reson Imaging* 2009; **30**: 327-334 [PMID: 19629981 DOI: 10.1002/jmri.21824]

28 **Papaevangelou E**, Almeida GS, Jamin Y, Robinson SP, deSouza NM. Diffusion-weighted MRI for imaging cell death after cytotoxic or apoptosis-inducing therapy. *Br J Cancer* 2015; **112**: 1471-1479 [PMID: 25880014 DOI: 10.1038/bjc.2015.134]

29 **Wang YC**, Hu DY, Hu XM, Shen YQ, Meng XY, Tang H, Li Z. Assessing the Early Response of Advanced Cervical Cancer to Neoadjuvant Chemotherapy Using Intravoxel Incoherent Motion Diffusion-weighted Magnetic Resonance Imaging: A Pilot Study. *Chin Med J* (Engl) 2016; **129**: 665-671 [PMID: 26960369 DOI: 10.4103/0366-6999.177995]

30 **Wang Z**, Su MY, Najafi A, Nalcioglu O. Effect of vasodilator hydralazine on tumor microvascular random flow and blood volume as measured by intravoxel incoherent motion (IVIM) weighted MRI in conjunction with Gd-DTPA-Albumin enhanced MRI. *Magn Reson Imaging* 2001; **19**: 1063-1072 [PMID: 11711230 DOI: 10.1016/S0730-725X(01)00431-3]

31 **Wirestam R**, Borg M, Brockstedt S, Lindgren A, Holtås S, Ståhlberg F. Perfusion-related parameters in intravoxel incoherent motion MR imaging compared with CBV and CBF measured by dynamic susceptibility-contrast MR technique. *Acta Radiol* 2001; **42**: 123-128 [PMID: 11281143 DOI: 10.1080/028418501127346459]

32 **Shinmoto H**, Tamura C, Soga S, Shiomi E, Yoshihara N, Kaji T, Mulkern RV. An intravoxel incoherent motion diffusion-weighted imaging study of prostate cancer. *AJR Am J Roentgenol* 2012; **199**: W496-W500 [PMID: 22997399 DOI: 10.2214/AJR.11.8347]

33 **Jensen JH**, Helpern JA. MRI quantification of non-Gaussian water diffusion by kurtosis analysis. *NMR Biomed* 2010; **23**: 698-710 [PMID: 20632416 DOI: 10.1002/nbm.1518]

34 **Shinmoto H**, Oshio K, Tanimoto A, Higuchi N, Okuda S, Kuribayashi S, Mulkern RV. Biexponential apparent diffusion coefficients in prostate cancer. *Magn Reson Imaging* 2009; **27**: 355-359 [PMID: 18768281 DOI: 10.1016/j.mri.2008.07.008]

P- Reviewer: Goetze TO, Martin-Villa JM, Zhang J **S- Editor**: Ma YJ
L- Editor: A **E- Editor**: Zhang DN

Published by **Baishideng Publishing Group Inc**
8226 Regency Drive, Pleasanton, CA 94588, USA
Telephone: +1-925-223-8242
Fax: +1-925-223-8243
E-mail: bpgoffice@wjgnet.com
Help Desk: http://www.wjgnet.com/esps/helpdesk.aspx
http://www.wjgnet.com

ISSN 1007-9327